Iranian Journal of Basic Medical Sciences
ijbms.mums.ac.ir

Advanced anti-aging strategy: Chitosan-coated albumin nanoparticles encapsulating metformin for enhanced therapeutic potential

Ghazal Farahnak [1#], Mona Alinia [1, 2#], Saeed Ghasemi [3], Mehdi Evazalipour [4], Ehsan Zamani [2], Saeed Manoochehri [1*]

[1] Department of Pharmaceutics, School of Pharmacy, Guilan University of Medical Sciences, Rasht, Iran
[2] Department of Pharmacology and Toxicology, School of Pharmacy, Guilan University of Medical Sciences, Rasht, Iran
[3] Department of Medicinal Chemistry, School of Pharmacy, Guilan University of Medical Sciences, Rasht, Iran
[4] Department of Pharmaceutical Biotechnology, School of Pharmacy, Guilan University of Medical Sciences, Rasht, Iran

ARTICLE INFO

Article type:
Original

Article history:
Received: Jul 7, 2026
Accepted: Nov 7, 2026

Keywords:
Aging
Albumins
Chitosan
Metformin
Nanoparticles
NIH 3T3 cells

ABSTRACT

Objective(s): Aging is a complex biological process marked by the progressive decline of cellular and systemic homeostasis, increasing the risk of chronic diseases, including diabetes, cardiovascular disorders, and neurodegenerative diseases. This study introduces a nanotechnology-based drug delivery platform comprising metformin-loaded bovine serum albumin (BSA) nanoparticles with a chitosan (CS) coating and evaluates its potential to counteract cellular senescence.

Materials and Methods: Nanoparticles were prepared by the desolvation method, which relies on solvent removal-induced nanoprecipitation. Formulation parameters were optimized to improve physicochemical stability. The biological efficacy of the formulation was evaluated in NIH/3T3 fibroblasts under experimentally induced oxidative stress.

Results: The mean particle size of nanoparticles was 217.1±23.6 nm, which is appropriate for endocytic uptake. The nanoparticles had an encapsulation efficiency of 89.93%, indicating efficient drug encapsulation. The zeta potential after chitosan coating was +46 mV, indicating improved colloidal stability. Treatment with the nanoparticles significantly reduced lipid peroxidation and restored intracellular glutathione levels, confirming antioxidative activity. In addition, the formulation also decreased senescence-associated β-galactosidase activity, suggesting its potential to mitigate cellular senescence.

Conclusion: Taken together, the results highlight the potential of metformin-loaded, chitosan-coated BSA nanoparticles as a targeted nanocarrier platform for age-related therapeutic interventions and underscore their importance in developing nanomedicine-based strategies.

▶ Please cite this article as:
Farahnak Gh, Alinia M, Ghasemi S, Evazalipour M, Zamani E, Manoochehri S. Advanced anti-aging strategy: Chitosan-coated albumin nanoparticles encapsulating metformin for enhanced therapeutic potential. Iran J Basic Med Sci 2027; 30:

Corrected Proof

Introduction

Aging is a natural biological process marked by a progressive decline in physiological function across multiple organ systems (1). It results from a combination of genetic and environmental factors. Aging is linked to chronic disorders, including diabetes, Alzheimer's disease, Parkinson's disease, cardiovascular disease, and osteoporosis (2). Understanding the complexity of aging is essential to developing innovative therapeutic strategies.

Cellular senescence is a critical mechanism that limits the proliferation and replication of damaged cells. It contributes to the molecular deterioration and cellular dysfunction underlying many age-related diseases (3).

Interventions for age-related conditions are diverse and include lifestyle modifications, gut microbiota modulation, cell replacement therapy, immunotherapy, and pharmacological strategies such as senolytics and antioxidants (1). Promising pharmacological interventions, including metformin, rapamycin, and ruxolitinib, have shown potential efficacy (1, 4).

Metformin is a compound derived from the French lilac plant and has glucose-lowering properties. It is used to treat type 2 diabetes (5). Additional effects include anti-inflammatory and immunomodulatory activity, modulation of gut flora, and reduced oxidative stress (5). It may delay aging and extend longevity by modulating key biological pathways, including insulin/IGF-1 signaling and activation of AMP-activated protein kinase (AMPK)(6).

Conventional metformin delivery is effective but is limited by low bioavailability, the need for frequent administration, and gastrointestinal adverse effects. (6, 7). Moreover, biological barriers that cause non-specific distribution and

*Corresponding author: Saeed Manoochehri. School of Pharmacy, Guilan University of Medical Sciences Campus, Guilan, Rasht, Iran. Tel/ Fax: +98-1333486475, Email: saeedmanoochehri@gmail.com
# These authors contributed equally to this work

© 2027. This work is openly licensed via CC BY 4.0.
This is an Open Access article distributed under the terms of the Creative Commons Attribution License (https://creativecommons.org/licenses), which permits unrestricted use, distribution, and reproduction in any medium, provided the original work is properly cited.

rapid drug clearance increase the complexity of systemic drug delivery (8). Therefore, researchers have developed novel delivery systems, particularly polymer-based systems, to improve treatment efficacy. Nanoscale carrier systems may enhance metformin bioavailability, reduce toxicity, and improve therapeutic efficacy (9, 10). This technology is promising for improving treatment modalities and contributing to interventions targeting age-related conditions (11, 12).

Albumin, a biocompatible plasma protein, is a promising material for nanoparticle formulations because of its biodegradability and ability to prolong drug circulation. Albumin-based nanoparticles improve drug stability and bioavailability and also exhibit therapeutic properties, including antioxidant and anti-inflammatory effects (13, 14).

The present study aimed to address these limitations by incorporating chitosan (CS), a well-known natural polymer with permeation-enhancing and mucoadhesive properties, into the nanoparticle formulation (14, 15). Because chitosan is positively charged and the cell membranes are negatively charged, electrostatic interaction may occur between the nanoparticles and the cell membrane surface. These interactions could increase nanoparticle residence time at the target site and improve drug delivery efficiency (16, 17).

In the present study, we have prepared Metformin (MET)-loaded, CS-coated Albumin nanoparticles. This formulation was designed to enhance cellular uptake, increase antioxidant activity, and potentially mitigate cellular aging processes (18). This novel nanoparticle formulation may offer new opportunities for anti-aging interventions and preserving cellular function.

Materials and Methods

Chemicals

Glutaraldehyde 25%, absolute ethanol, sodium hydroxide (NaOH), sodium chloride (NaCl), potassium ferricyanide, potassium ferrocyanide, magnesium chloride ($MgCl_2$), potassium chloride (KCl), disodium hydrogen phosphate (Na_2HPO_4), hydrochloric acid (HCl), Trypsin, Coomassie Blue, methanol, phosphoric acid, monobasic potassium phosphate, formaldehyde, dimethylformamide, sulfuric acid, n-butanol, 5,5′-dithiobis(2-nitrobenzoic acid) (DTNB), and glutathione powder were obtained from Merck, Germany. Bovine serum albumin (BSA; ≥99%), low molecular weight chitosan (50-190kDa), phosphate-buffered saline (PBS), X-gal, sucrose, Tris-HCl, thiobarbituric acid (TBA), cytochalasin B, tetramethoxypropane, ethylenediaminetetraacetic acid (EDTA), trichloroacetic acid (TCA), Tris ammonium, and sodium acetate were purchased from Sigma Chemical Company (USA). Metformin hydrochloride and acetic acid were purchased from Mahban Shimi and Mojalali, Iran, respectively. The NIH/3T3 cell line was obtained from the National Cell Bank of the Pasteur Institute (Tehran, Iran). Dulbecco's modified Eagle Medium (DMEM), fetal bovine serum (FBS), and the antibiotic/antimycotic solution were obtained from Bioidea, Iran. The fetal bovine serum (FBS) was obtained from Invitrogen. All other reagents and solvents used were of analytical grade.

Preparation of nanoparticles

Preparation of metformin-loaded BSA nanoparticles

To prepare metformin-loaded BSA nanoparticles, 50 mg of BSA was dissolved in 5 ml of distilled water. Next, 10 mg of metformin (MET) was added incrementally to the aqueous BSA solution. The solution was then refrigerated at 4 ˚C for 24 hr. The pH was adjusted to 8-9. The solution was agitated for 10 min at room temperature to reach equilibrium. Subsequently, absolute ethanol was intermittently added dropwise to the aqueous solution at 5-min intervals until a faint blue turbidity was observed. After a 30-min incubation with absolute ethanol, 25 µl of an 8% (v/v) glutaraldehyde solution was added to harden the desolvated MET-loaded BSA nanoparticles. The solution was stirred at room temperature for 12 hr. Finally, the solvent was evaporated at 40 ˚C using an incubator shaker. The nanoparticles were purified by centrifugation at 20,000 rpm for 15 min at 25 ˚C. The resulting nanoparticles were washed with purified water and centrifuged again. The purified nanoparticles were then redispersed in 5 ml of water for subsequent experiments (19). We additionally prepared blank BSA nanoparticles using the same procedure.

Preparation of metformin-loaded, chitosan-coated BSA nanoparticles

For the preparation of metformin-loaded chitosan-coated BSA nanoparticles, metformin-loaded BSA nanoparticles were prepared as described above, with some modifications. At this stage, 50 mg BSA and 10 mg metformin were dissolved in 5 ml of 10 mM NaCl solution instead of water, then stored at 4 ˚C for 24 hr (20).

Finally, the synthesized BSA-MET-NPs (metformin-loaded bovine serum albumin nanoparticles) were added to a chitosan-acetic acid solution (1 mg/ml, pH 4.5) at a 1:1 ratio (total chitosan content: 5 mg). The mixture was agitated for 15 min. Figure 1 presents a schematic representation of the nanoparticle preparation process (20).

In vitro characterization of the nanoparticles

Particle size and zeta potential

The particle size and polydispersity index (PDI) of the nanoparticles were determined using a Microtrac Nanotrac Flex instrument (Haan/Düsseldorf, Germany) based on dynamic light scattering. The zeta potential of the nanoparticles was measured using a Stabino Zeta instrument coupled with the Nanotrac Flex (Haan/Düsseldorf, Germany).

Evaluation of nanoparticle morphology

The size and morphology of BSA-MET-NPs, BSA-MET-CS-NPs, and bovine serum albumin nanoparticles (BSA-NPs) were examined by transmission electron microscopy (TEM) using a Zeiss microscope (Germany). The surface characteristics of the nanoparticles were further examined by field-emission scanning electron microscopy (FESEM).

FT-IR analysis

Fourier-transform infrared (FT-IR) spectroscopy was employed to examine the functional groups of the synthesized BSA-MET-NPs and BSA-MET-CS-NPs. Spectra were obtained using an attenuated total reflectance Fourier-transform infrared (ATR-FT-IR) spectrometer (PerkinElmer, Germany) over a wavenumber range of 450-4000 cm^{-1}. Each spectrum represented the average of 16 scans.

Determination of encapsulation efficiency (EE%) and loading capacity (LC)

The drug encapsulation efficiency was determined by an

Corrected Proof

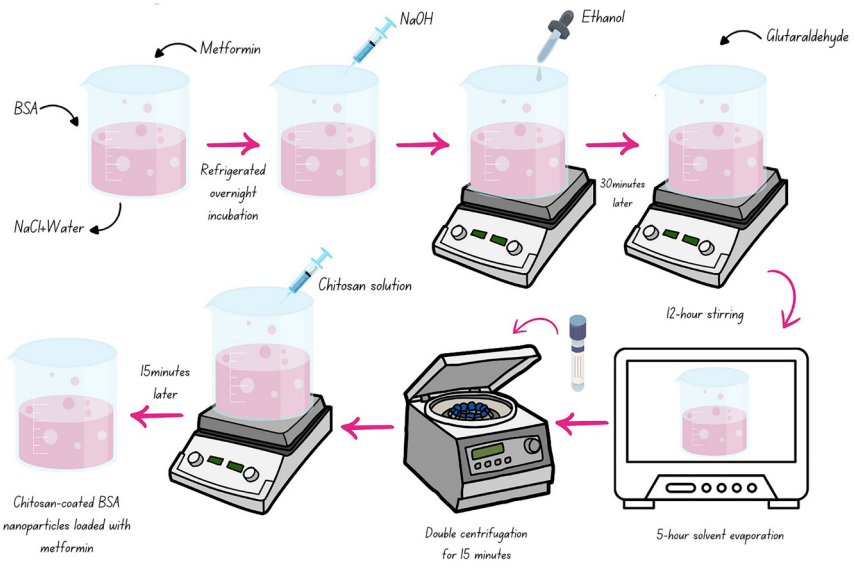


Figure 1. Schematic illustration of the preparation of metformin-loaded, chitosan-coated bovine serum albumin nanoparticles

indirect analytical method. The supernatant was collected by centrifugation and filtered through a 0.45-µm syringe filter. The filtrate was diluted, and its absorbance was measured with a UV-visible spectrophotometer (Lambda 25, PerkinElmer, USA). The encapsulation efficiency (EE) and drug loading capacity (LC) were then calculated using the following equations:

Encapsulation Efficiency (%)=(Initial amount of MET-Free MET in supernatant)/(Initial amount of MET)×100

Loading Capacity (%)=(Initial amount of MET-Free MET in supernatant)/(Total amount of initial MET and BSA@)×100

Cell culture and treatment

NIH/3T3 cells at the third passage were inoculated at a density of 1.9×10^5 cells per well in 6- and 12-well plates and incubated in a humidified environment containing 5% CO_2 at 37 ˚C. Afterward, these cells were penetrated for 24 hr with different concentrations (250 µM, 1 mM, and 4 mM) of BSA-MET-CS-NPs (BMC-NPs). Cells were subsequently plated in 6-well plates for β-galactosidase assays and in 12-well plates for oxidative stress experiments at densities of 2×10^4 and 2×10^5 cells per well, respectively. The cells were segregated into the following experimental groups:

- Group 1: (Control): NIH/3T3 cells cultured in DMEM-HG medium
- Group 2: Blank NP: Chitosan-Coated BSA Nanoparticles
- Group 3: (H_2O_2): NIH/3T3 cells treated with H_2O_2 (400 µM)
- Group 4: Metformin (4 mM) + H_2O_2
- Group 5: Metformin-Loaded, Chitosan-Coated BSA Nanoparticles (BMC3; 4 mM; blank NP)
- Group 6: Metformin-Loaded, Chitosan-Coated BSA Nanoparticles (BMC1; 250 µM) + H_2O_2
- Group 7: Metformin-Loaded, Chitosan-Coated BSA Nanoparticles (BMC2; 1 mM) + H_2O_2
- Group 8: Metformin-Loaded, Chitosan-Coated BSA Nanoparticles (BMC3; 4 mM) + H_2O_2

β-Galactosidase assays

Senescence-associated β-galactosidase (SA-β-gal) staining assay

To identify senescent cells, we measured β-galactosidase activity, which is detectable in these cells at pH 6. Cultured cells were inoculated into 6-well plates and treated according to prior methodology. After the treatment, the cells were thoroughly washed with phosphate-buffered saline (PBS). The specimens were subsequently fixed for 5 min at ambient temperature in a solution containing 20% formaldehyde and 2% glutaraldehyde. After fixation, the cells were rinsed with PBS to remove any remaining fixatives. The cells were stained with X-gal solution and incubated at 37 ˚C for 12-16 hr. The presence of senescent cells was confirmed by observing blue-green staining under a microscope at 200× magnification (21).

Quantification of oxidative stress parameters

Assessment of lipid peroxidation

To assess the extent of lipid peroxidation, malondialdehyde (MDA) levels were measured using a modified TBA assay. Cell homogenates were mixed with 0.25 ml of sulfuric acid (0.05 M) and 0.3 ml of TBA (0.2%). The mixtures were incubated for 60 min in a boiling water bath. After incubation, the mixture was immediately cooled on ice, and n-butanol was added uniformly to all samples. The mixtures were centrifuged at 3500 ×g for 10 min, and supernatant absorbance was measured in triplicate on an ELISA microplate reader at 532 nm. MDA concentrations were calculated from a standard curve and reported as micromolar (µM) concentrations (22, 23).

Assessment of glutathione content

Glutathione content was determined with minor modifications to established methods. To assess glutathione, 5,5'-dithiobis(2-nitrobenzoic acid)(DTNB) was used as an indicator. Proteins were precipitated by treatment of cell suspensions with trichloroacetic acid (TCA). Then, the cells were centrifuged at 5000 ×g for 5 min at 4 ˚C. The supernatants from each group were first mixed with

Corrected Proof

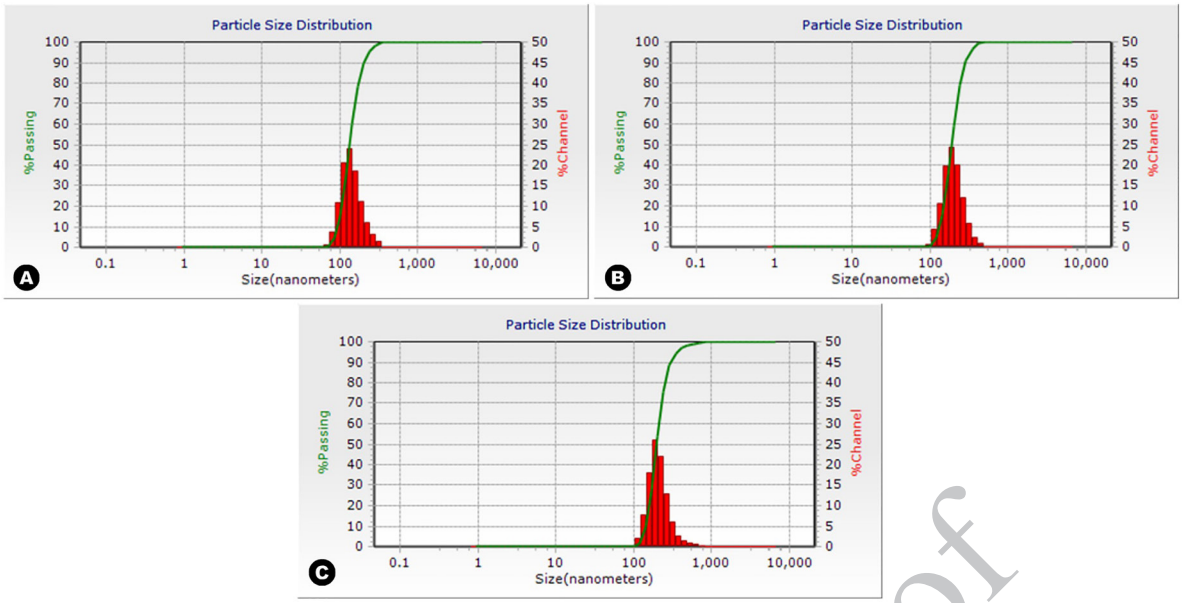


Figure 2. Particle size distribution of Nanoparticles
A) Bovine serum albumin nanoparticles B) Metformin-loaded bovine serum albumin nanoparticles, C) Metformin-loaded, chitosan-coated BSA nanoparticles

phosphate-buffered saline (PBS; 0.2 M, pH 7.6) and then with DTNB (0.001 M). The glutathione concentration was quantified from the absorbance of the samples at 412 nm using a spectrophotometer. Total glutathione was calculated from a standard curve, and results were expressed as micromolar (μM) concentrations (24).

Statistical analysis

Data are presented as mean±standard deviation (SD). Data were statistically analyzed using one-way analysis of variance (ANOVA), followed by Tukey's *post hoc* test, using SPSS version 13. The graphs were generated using Prism version 6. Each experiment was performed in triplicate, and the mean of the triplicates was used for statistical analysis. A *P*-value<0.05 was considered statistically significant.

Results

Characterization of the synthesized BSA nanoparticles

Zeta potential and DLS analysis

The Bovine serum albumin nanoparticles (BSA-NPs) had a particle size of 144.4±18.3 nm and a polydispersity index (PDI) of 0.5. Moreover, the nanoparticles had a zeta potential of -144.3 mV, indicating high electrostatic stability. After adding metformin, the particle size increased to 202 nm, while the PDI remained at 0.5, indicating that the size distribution remained acceptable. The zeta potential shifted considerably toward neutrality at 0.2 mV, indicating a substantial loss of electrostatic stability. BSA-MET-CS-NPs had a higher particle size of 217.1±23.6 nm and a slightly higher PDI of 0.6, indicating a broader size distribution. The zeta potential shifted to +46.0 mV, indicating improved colloidal stability. Figure 2 shows the particle size distribution of the different nanoparticle formulations. A high absolute zeta potential can improve formulation stability by preventing aggregation through electrostatic repulsion. The positive surface charge of CS-coated BSA nanoparticles may also facilitate their interaction with negatively charged cell membranes. Table 1 presents particle size, PDI, and zeta potential data.

FT-IR analysis

FT-IR analysis was used to assess the surface chemical composition of the chitosan-coated albumin nanoparticles. Comparison of the FT-IR spectra of chitosan-coated and uncoated nanoparticles (Figure 3) provided significant information about structural changes induced by the chitosan coating. The FT-IR spectrum of uncoated nanoparticles showed a characteristic peak at 3276 cm^{-1}, corresponding to O-H stretching vibrations of alcohols and N-H stretching vibrations of primary amines and amide groups. The band at 2959 cm^{-1} was attributed to C-H stretching in aliphatic molecules. The second peak at 1635 cm^{-1} was assigned to C=O stretching in amide groups.

In the spectra of the chitosan-coated nanoparticles, the peaks shifted and increased in intensity. Prominent peaks appeared at 3279 cm^{-1} (O-H and N-H stretching vibrations),

Table 1. The particle size, polydispersity index (PDI), and zeta potential of nanoparticles

Nanoparticles	Particle size	Polydispersity index (PDI)	Zeta potential
BSA-NPs	144.4±18.3 nm	0.5	-144.3 mV
BSA-MET-NPs	202.2±14.6 nm	0.5	0.2 mV
BSA-MET-CS NPs	217.1±23.6nm	0.6	46 mV

BSA-NPs: Bovine serum albumin nanoparticles, BSA-MET-NPs: metformin-loaded bovine serum albumin nanoparticles, BSA-MET-CS-NPs: Metformin-loaded, chitosan-coated bovine serum albumin nanoparticles

Corrected Proof

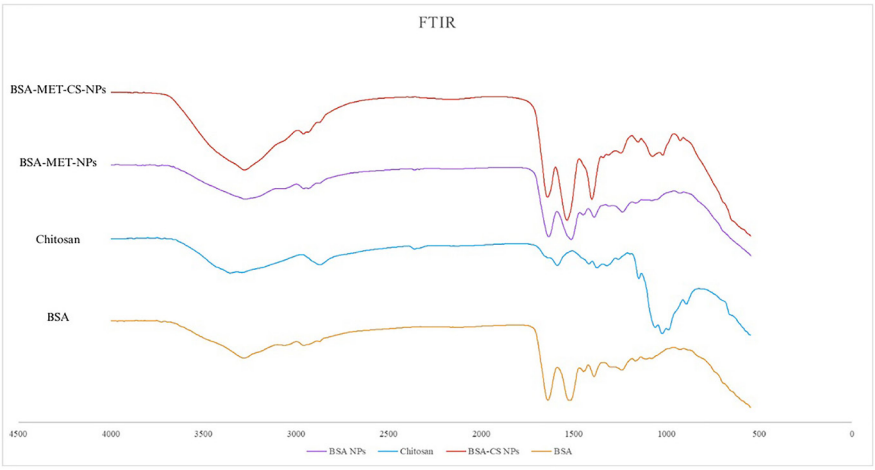


Figure 3. FT-IR spectra of A) BSA-MET-NPs: Metformin-loaded bovine serum albumin nanoparticles, B) BSA-MET-CS-NPs: Metformin-Loaded, chitosan-coated bovine serum albumin nanoparticles

2960 cm^{-1} (C-H stretching vibration), and 1643 cm^{-1} (C=O stretching vibration). New peaks appeared at 1537 cm^{-1} (C-N stretching and N-H bending vibrations) and at 1403 cm^{-1} and 1343 cm^{-1} (methyl bending adjacent to the amide carbonyl and amide III deformation, respectively). The peaks at 1076 cm^{-1} and 1020 cm^{-1}, which are characteristic of C-O stretching in ethers and alcohols, further supported the incorporation of chitosan ether functional groups into the nanoparticle matrix.

The prominent peak at 3279 cm^{-1} in the chitosan-coated nanoparticles supported the incorporation of amino and hydroxyl groups into the nanoparticle framework. The increased intensity at 1643 cm^{-1} in chitosan-coated samples indicated a significant contribution of C=O functional groups. The single peak at 1537 cm^{-1} and the absence of peaks at 1403 and 1343 cm^{-1} in the uncoated nanoparticles suggested chitosan-induced structural changes. The C-O stretching vibrations at 1076 and 1020 cm^{-1} were also consistent with the incorporation of chitosan ether groups into the nanoparticle matrix.

Table 2 presents the FT-IR peak assignments for BSA-MET-NPs and BSA-MET-CS-NPs, which collectively support successful chitosan coating.

Comparative SEM and TEM analysis of nanoparticles

Structural insights and morphological characterization

FESEM analysis showed that the bovine serum albumin nanoparticles were predominantly spherical and uniformly coated with chitosan. TEM analysis showed, consistent with the FESEM results, that the nanoparticles were uniformly distributed and generally retained a spherical morphology, with slight size variations. TEM also confirmed a chitosan shell around the nanoparticles, resulting in larger diameters than those of the uncoated nanoparticles. Meanwhile, the chitosan coating led to the formation of a special shell on the surface. Figure 4 presents the FESEM and TEM images.

Metformin content and drug encapsulation efficiency (EE%)

Metformin drug loading, defined as the percentage of metformin encapsulated within the nanoparticles relative to the total weight of nanoparticles, was 14.46% for BSA-MET-NPs and 13.82% for BSA-MET-CS-NPs. Encapsulation efficiency, defined as the percentage of metformin encapsulated within the nanoparticles relative to the initial weight of metformin, was 86.80% and 89.93% for BSA-MET-NPs and BSA-MET-CS-NPs, respectively.

Corrected Proof

Table 2. FT-IR analysis of metformin-loaded bovine serum albumin nanoparticles (BSA-MET-NPs) and metformin-loaded, chitosan-coated bovine serum albumin nanoparticles (BSA-MET-CS-NPs)

Absorption peak(cm^{-1})		Assignment
BSA-MET-NPs	BSA-MET-CS-NPs	
3276	3279	O-H alcoholic, N-H amine I, N-H amide I stretching vibrations
2959	2960	C-H aliphatic stretching vibrations
1635	1643	C=O stretching vibration of amides
-	1537	Combination of C-N Tension Bar and N-H Bending Bar
-	1403	Bending vibrations of a methyl group attached to an amide carbonyl
–	1343	The amide III bond is related to the deformation of the amide NH
–	1076	C-O etheric stretching vibration
–	1020	C-O alcoholic stretching vibration

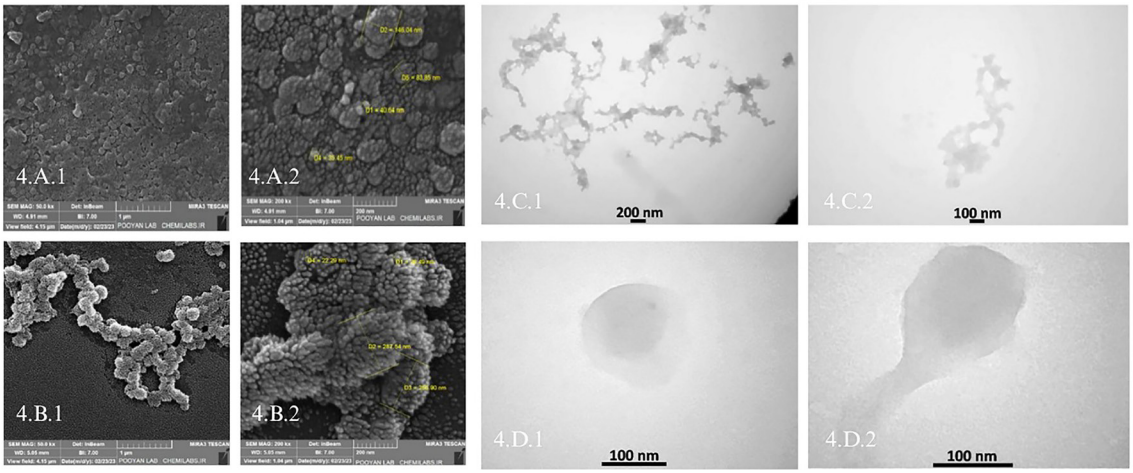


Figure 4. SEM and TEM images of nanoparticles
4.A.1) BSA-MET-NPs: Metformin-loaded bovine serum albumin nanoparticles (1µm), 4.A.2) BSA-MET-NPs: Metformin-loaded bovine serum albumin nanoparticles (200 nm), 4.B.1) BSA-MET-CS-NPs: Metformin-loaded, chitosan-coated bovine serum albumin nanoparticles (1µm), 4.B.2) BSA-MET-CS-NPs: Metformin-loaded, chitosan-coated bovine serum albumin nanoparticles (200nm), TEM images of nanoparticles. 4.C.1) BSA-MET-NPs: Metformin-loaded bovine serum albumin nanoparticles (200 nm) 4.C.2) BSA-MET-NPs: Metformin-loaded bovine serum albumin nanoparticles (100 nm) 4.D.1) BSA-MET-CS-NPs: Metformin-loaded, chitosan-coated bovine serum albumin nanoparticles (100 nm) 4.D.2) BSA-MET-CS-NPs: Metformin-loaded, chitosan-coated bovine serum albumin nanoparticles (100 nm)

Results of the SA-β-Gal staining assay

Figure 5 shows the effects of BSA-MET-NPs, BSA-MET-CS-NPs, MET, and H_2O_2 on β-galactosidase activity. After H_2O_2 treatment, β-galactosidase activity increased significantly, and a distinct blue-green color was observed compared with the control group. Treatment with BSA-MET-NPs, BSA-MET-CS-NPs, and MET reduced β-galactosidase activity. However, the reduction with MET was less pronounced than that observed with MET-containing nanoparticle formulations.

Oxidative stress parameters

Lipid peroxidation assay

As shown in Figure 6, MDA concentrations were significantly higher in the H2O2-treated group than in the control group (P<0.001). MDA levels were significantly lower in the BMC1- and BMC2-treated groups than in the H2O2-treated group (P<0.001). MET treatment improved MDA levels but not as effectively as the BSA-NPs treatments. Therefore, the BSA-MET-CS-NPs (BMC) may protect against H_2O_2-induced oxidative damage.

Glutathione content measurement

As shown in Figure 7, glutathione (GSH) concentrations were significantly lower in the H_2O_2-exposed groups than in the control group (P<0.01). In contrast, GSH levels in the BSA-MET-CS (BMC)- treated groups increased significantly relative to the H_2O_2-treated group (P<0.001). Furthermore, while MET elevated GSH levels, this effect was less pronounced than with the BSA-MET-CS-NPs treatments. No statistically significant differences were observed among the BMC-treated groups in GSH concentration increases.

Corrected Proof

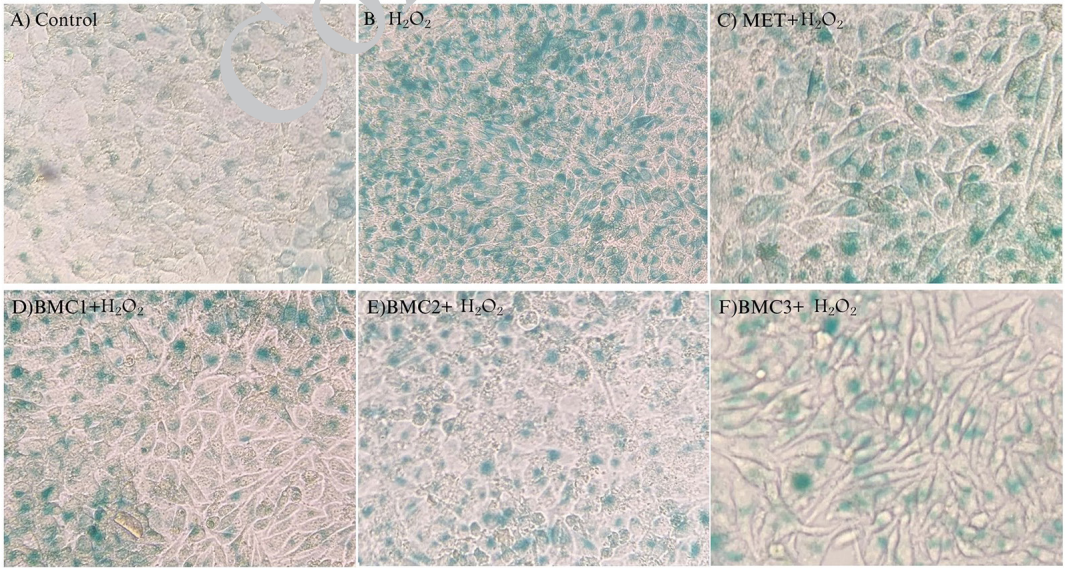


Figure 5. β-galactosidase staining assay in embryonic fibroblast cells
A) Control. B) H_2O_2: treated with H_2O_2 at 400 µM. C) MET+H_2O_2: treted with metformin at 4 mM+H_2O_2. D) BMC1+H_2O_2: treated with Metformin-loaded chitosan-coated bovine serum albumin nanoparticles at 250 µM+H_2O_2. E) BMC2+H_2O_2: treated with metformin-loaded chitosan-coated bovine serum albumin nanoparticles at 1 mM+H_2O_2. F) BMC3+H_2O_2: treated with metformin-loaded chitosan-coated bovine serum albumin nanoparticles at 4 mM+H_2O_2

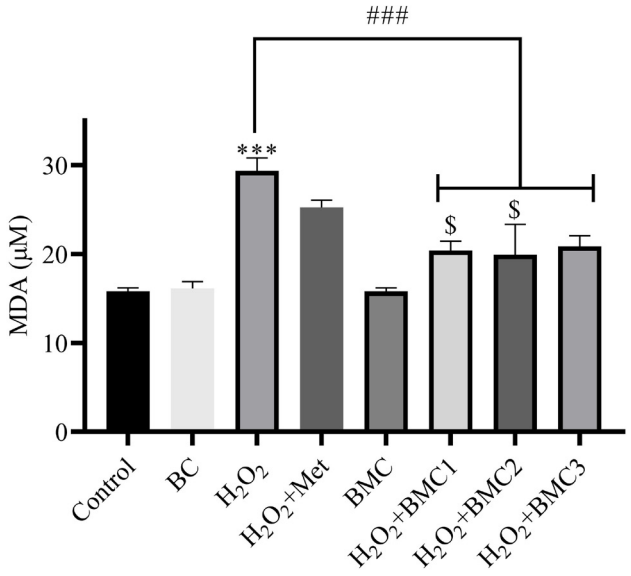


Figure 6. The effect of metformin and nanoparticles on lipid peroxidation in the NIH.3T3 cells after H_2O_2 (400 µM) exposure
BC: Chitosan-coated bovine serum albumin nanoparticles, MET: metformin at 4 mM, BMC: Metformin-loaded chitosan-coated bovine serum albumin nanoparticles at 4 mM. BMC1: Metformin-loaded chitosan-coated bovine serum albumin nanoparticles at 250 µM, BMC2: Metformin-loaded chitosan-coated bovine serum albumin nanoparticles at 1 mM. BMC3: Metformin-loaded chitosan-coated bovine serum albumin nanoparticles at 4 mM. $^{***}P<0.001$, significantly different from the Control group. $^{###}P<0.001$, significantly different from the H2O2 group. $^{\$}P<0.05$ significantly different from the Met+H_2O_2 group

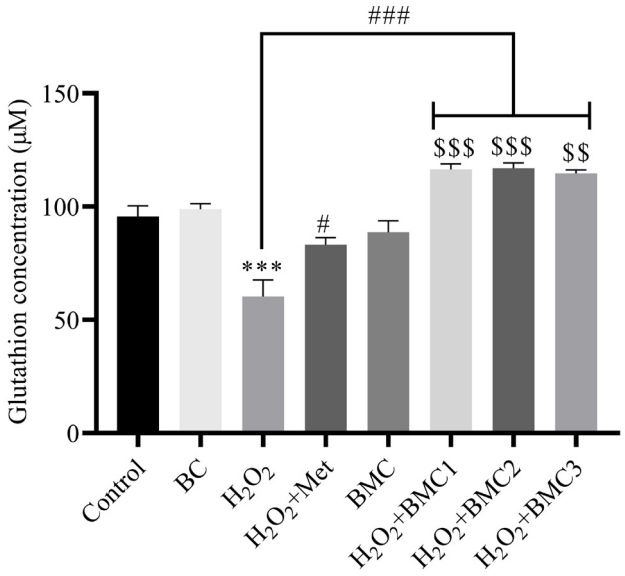


Figure 7. The effect of metformin and nanoparticles on glutathione concentration in the NIH.3T3 cells H_2O_2 (400 µM) exposure
BC: Chitosan-coated bovine serum albumin nanoparticles, MET: Metformin at 4 mM, BMC: Metformin-loaded chitosan-coated bovine serum albumin nanoparticles at 4 mM. BMC1: Metformin-loaded chitosan-coated bovine serum albumin nanoparticles at 250 µM, BMC2: Metformin-loaded chitosan-coated bovine serum albumin nanoparticles at 1 mM. BMC3: Metformin-loaded chitosan-coated bovine serum albumin nanoparticles at 4 mM.$^{***}P<0.001$, significantly different from the Control group. $^{###}P<0.001$, significantly different from the H_2O_2 group. $^{\#}P<0.05$ significantly different from the H_2O_2 group. $^{\$\$\$}P<0.001$, significantly different from the Met+H_2O_2 group. $^{\$\$}P<0.01$, significantly different from the Met+H_2O_2 group

Discussion

Aging is a complex biological process marked by the progressive deterioration of physiological functions due to the accumulation of cellular and molecular damage. Cellular senescence is a major contributor to this decline and is associated with chronic disorders such as diabetes, Alzheimer's disease, and cardiovascular disease. Recent research suggests that some interventions, such as lifestyle modification and drugs such as metformin, may delay aging and extend lifespan (25, 26). To overcome the limitations of conventional therapies, researchers are designing nanoparticle-based drug delivery systems to improve stability, bioavailability, and targeted distribution, thereby improving treatment outcomes and quality of life (27-30).

This research focused on preparing metformin-loaded, chitosan-coated BSA nanoparticles as a novel drug-delivery vehicle. Nanoparticles are prepared to overcome the problems of drug delivery and enhance drug action. Significant research has investigated the anti-aging effects of albumin nanoparticles under oxidative stress conditions (a cause of aging). The results indicated that Metformin-Loaded, Chitosan-Coated BSA Nanoparticles are a novel anti-aging agent with promising potential for future applications.

After successfully developing a suitable formulation, the synthesized nanoparticles were characterized for their physicochemical properties. Reducing particle size is a main reason for enhanced cellular uptake of nanoparticles. The nanoparticle dimensions at each stage were analyzed using Dynamic Light Scattering (DLS).

The blank BSA-NPs showed an initial average particle size of 144.4±18.3 nm. Subsequently, albumin nanoparticles encapsulating metformin were prepared. Throughout this process, the size and zeta potential of the nanoparticles increased with the metformin loading, while the polydispersity index remained unchanged. These data support Mingping He's finding that nanoparticle size increases upon drug loading. The hydration kinetic diameter of BSA nanoparticles encapsulating liraglutide increased from 28.2 nm to 32.7 nm (31). These results are consistent with Salim *et al.*, in which the diameter of albumin nanoparticles loaded with gemcitabine increased from 100 nm to 170 nm (32). Thus, nanoparticle loading can alter their size (33).

The zeta potential of BSA nanoparticles with and without metformin differed significantly, indicating the drug's effect on stability. Therefore, the metformin-encapsulated albumin nanoparticles were coated with chitosan to enhance their stability. This coating was essential for stabilizing the nanoparticles and served as a basis for further modification to optimize the physicochemical properties and to assess their potential anti-aging benefits (32, 34).

In the present study, chitosan was used as a coating material to address this issue. The zeta potential of the coated nanoparticles was increased to +46 mV. This was done by increasing the particle size to 217.1±23.6 nm and inverting the zeta potential to positive values, as reported in previous studies (35-37). The increase in zeta potential from the amine groups of the chitosan polymer shows that there are successful electrostatic interactions between the albumin nanoparticles (which are negatively charged) and the chitosan (which is positively charged) (38, 39).

The same trend was observed in Taherian's study, where the size of uncoated magnetic nanoparticles increased from 30.3 ± 7.1 nm to 34.2 ± 8.4 nm after chitosan coating. The observed increase in size and positive zeta potential in the study signifies successful electrostatic interactions that

Corrected Proof

enhance the stability of nanoparticle suspensions (36).

Other studies further support chitosan's effectiveness in enhancing nanoparticle stability. For example, Salim *et al.* observed an increase in particle size from 170 nm to 200 nm after chitosan coating, consistent with the present study's findings (33). Aligns with the findings of the current investigation. Radwan *et al.* showed a notable increase in zeta potential from −29 mV to 24 mV after chitosan coating of albumin nanoparticles, illustrating the coating's efficacy (40). These findings align with our studies, showing that the zeta potential of chitosan-coated nanoparticles consistently exceeded +46 mV, indicating enhanced stability and reduced aggregation.

Bessone *et al.* reported an increase in zeta potential from -28.9 mV to 8 mV after coating doxorubicin-loaded albumin nanoparticles with glycol chitosan (41). The change in surface charge further supports the effect of chitosan coating on nanoparticle stability, confirming the result of the present study.

The FT-IR analysis is consistent with the methods followed in the study by Yourui Li, demonstrating a well-defined interaction between chitosan and albumin (42).

The morphological characterization of BSA-NPs used different electron microscopy techniques to demonstrate fundamental structural features. The FESEM study showed that both BSA-MET-NPs and BSA-MET-CHI-NPs were predominantly spherical, as reported in a previous study. Jose *et al.* reported that albumin nanoparticles maintain their spherical shape when metformin is encapsulated (43). In our FESEM analysis, the chitosan-coated layer maintained the outer shell's consistency and regularity. Jose *et al.* and Piazzini *et al.* reported similar outcomes, noting the development of a unique chitosan shell on the nanoparticle surface, which increased stability and functionality (20, 43).

TEM analysis confirmed the FESEM data, revealing uniformly dispersed nanoparticles with a spherical morphology and a polydisperse size distribution. TEM also confirmed a chitosan shell around the nanoparticles, indicating that the coated nanoparticles had larger diameters than their uncoated counterparts. This data aligns with Salim *et al.*'s study, which showed that gemcitabine accumulation in chitosan-coated nanoparticles increased particle size (33). Similarly, Li *et al.* and Bessone *et al.* reported that increased diameters of chitosan-coated albumin nanoparticles were due to the chitosan layer (41, 42). This aligns with Piazzini *et al.*, who indicated that the chitosan coating created a distinct layer on the nanoparticle surface, enhancing nanoparticle stability and functionality (38).

This outcome confirmed the findings of Radwan *et al.*, who also observed the development of a spherical chitosan halo surrounding albumin nanoparticles (40). The increase in chitosan-coated nanoparticle size, along with the successful and uniform application of the chitosan layer, is essential for improving drug-delivery capabilities.

Our research demonstrated a consistent and effective chitosan coating, suggesting that these nanoparticles may have improved stability, an important factor for potential therapeutic applications. The findings support the concept that chitosan coating, although it increases nanoparticle size, enhances structural integrity, thereby optimizing them for drug delivery applications.

The drug loading of metformin in BSA-MET-NPs and BSA-MET-CS-NPs was determined to be 14.46% and 13.82%, respectively. The encapsulation efficiencies for BSA-MET-NPs and BSA-MET-CS-NPs were 86.80% and 89.93%, respectively. The elevated encapsulation efficiencies observed in this investigation align with the studies in the literature. Mahmoud Hasan showed that chitosan coating of nanoliposomes markedly increased curcumin encapsulation efficiency from 78.2±0.5% to 95.2±1.2% (44). In a separate investigation, curcumin nanoliposomes synthesized via the ethanol injection method had an encapsulation efficiency of 54.7%, which improved to 64.9% upon coating with 0.1% chitosan, as reported by Shin *et al.* (45). The elevated drug loading and encapsulation efficiency of chitosan-coated BSA-metformin nanoparticles (BSA-MET-CS-NPs) are presumably attributable to several physicochemical interactions. The positive charge of chitosan facilitates electrostatic interaction with the negatively charged BSA surface, creating a highly stable interfacial barrier that restricts drug dispersion during formulation (46). The coating serves as a diffusion barrier, hence decreasing porosity and enhancing drug entrapment (47). Moreover, hydrogen bonding among the functional groups of chitosan, metformin, and BSA can enhance drug retention (48). This may be attributed to the elevated viscosity of the chitosan-containing medium and limited nanoparticle compaction, which enhances encapsulation efficiency (49).

Senescence is a recognized cellular condition marked by the permanent cessation of the cell cycle. This process is essential to the biological mechanics of aging. Numerous biomarkers have been proposed to identify senescent cells in experimental models, with senescence-associated β-galactosidase (SA-β-gal) activity proving highly specific and reliable. SA-β-gal refers to enzymes that catalyze the hydrolysis of non-reducing β-D-galactose residues from β-D-galactosyl substrates, including glycoproteins, keratan sulfate, and sphingolipids. Overexpressing β-galactosidase may increase β-galactosidase activity in senescent cells under suboptimal pH conditions. Nonetheless, the enzymatic activity is significantly diminished in actively growing cells (50).

Oxidative stress is a mediating causative agent in the chemically induced cellular damage observed in divers, with key manifestations including DNA strand breaks, enzyme inactivation, and heightened lipid peroxidation levels (LPO). LPO is a primary mechanism underlying the harmful effects of many xenobiotics. In this process, unsaturated fatty acids, primarily found in biological membranes, become vulnerable to oxidation by oxygen-derived radicals, resulting in irreversible cellular damage. MDA, a significant product of lipid peroxidation (LPO), can interact with and inactivate many macromolecules, ultimately leading to cellular death. The MDA concentrations in the BMC1 and BMC2 treatment groups were considerably lower than those in the H_2O_2 and MET+H_2O_2 groups. This suggests that BMC1 and BMC2 may protect against H2O2-induced oxidative stress. A study by Salma El-Sayed Radwan showed that CS-TET-BSA-NPs (chitosan tetrandrine bovine serum albumin nanoparticles) significantly reduced MDA levels compared with the control groups, supporting the efficacy of these nanoparticle formulations in mitigating oxidative damage (40).

The amounts of glutathione (GSH) in the BSA-MET-C (BMC) treatment groups were statistically elevated relative

Corrected Proof

to the H_2O_2 and MET+H_2O_2 groups. Furthermore, no statistically significant differences were seen in the rise in GSH concentrations among the BMC-treated groups. Statistical analysis showed no significant difference in the increase in cellular glutathione levels and MDA between the nanoformulation groups and the control group. This pattern may reflect reduced basal cellular oxidation. Research by Elsayed I. Salim *et al*. showed elevated glutathione levels in the MCF-7 cancer cell line after treatment with gemcitabine-loaded albumin nanoparticles coated with chitosan (33).

This drug delivery system employs a multifaceted approach by integrating many modes of action. It includes albumin's antioxidant properties, chitosan's antioxidative and anti-inflammatory effects, the potential for targeted drug delivery via nanoparticles, and chitosan's improved cellular absorption due to its positive charge. Together, these features may reduce reactive oxygen species (ROS) generation (51-55). Albumin has antioxidant capabilities that enable it to sequester free radicals, thereby protecting against oxidative damage effectively. Chitosan's protective effects against oxidative stress are reflected in decreased ROS production and improved antioxidant enzyme activity. Moreover, delivering drugs using albumin nanoparticles to target sites reduces drug interactions in non-target tissues, leading to less free-radical generation in non-target areas (56). ROS generation can be altered by metformin through various pathways, thus reducing oxidative stress. Therefore, combining these ingredients may significantly reduce MDA levels and increase intracellular glutathione, reducing subsequent damaging effects (57).

Conclusion

This study highlights the potential of metformin-loaded bovine serum albumin nanoparticles coated with chitosan (BSA-MET-CS-NPs) as a novel drug delivery system to mitigate aging-associated oxidative stress and cellular senescence. Metformin-loaded bovine serum albumin nanoparticles coated with chitosan showed remarkable stability, higher drug encapsulation efficiency, and improved cellular interactions due to chitosan incorporation. Reduced oxidative stress and cellular senescence indicators *in vitro* suggest that these NPs are preferable to free metformin.

Although this drug delivery system improved certain markers of oxidative stress and cellular senescence, the present study evaluated only a limited number of cellular senescence markers. Therefore, future studies should investigate additional markers of cellular senescence beyond β-galactosidase to obtain more comprehensive data. Furthermore, this delivery system may be promising for treating age-associated diseases; however, further studies are needed in a live animal model.

Acknowledgment

The results presented in this paper were part of two Pharm.D. theses. They were supported by the Research Council of Guilan University of Medical Sciences, Rasht, Iran (Ethical codes: IR.GUMS.REC.1401.131 and IR.GUMS.REC.1403.158). The authors thank Ms. Saberi, the laboratory staff, and everyone who helped with this research.

Authors' Contributions

G F and M A wrote the original draft and contributed to the investigation and methodology. S G contributed to writing, review and editing, formal analysis, and validation. M E conducted the formal analysis and contributed to the methodology and validation. E Z contributed to writing, review and editing, supervision, and conceptualization. S M contributed to writing, review and editing, supervision, project administration, and conceptualization.

Conflicts of Interest

The authors declare that they have no known competing financial interests or personal relationships that could have influenced the work reported in this paper.

Declaration

We acknowledge the use of ChatGPT (OpenAI) for language editing as well as minor text revisions.

References

1. Guo J, Huang X, Dou L, Yan M, Shen T, Tang W, *et al.* Aging and aging-related diseases: from molecular mechanisms to interventions and treatments. Signal Transduct Target Ther 2022; 7: 391.
2. Abourehab MA, Pramanik S, Abdelgawad MA, Abualsoud BM, Kadi A, Ansari MJ, *et al.* Recent advances of chitosan formulations in biomedical applications. Int J Mol Sci 2022; 23: 10975.
3. Ogrodnik M. Cellular aging beyond cellular senescence: Markers of senescence prior to cell cycle arrest *in vitro* and *in vivo*. Aging Cell 2021; 20: e13338.
4. Zhang X-X, He S-H, Liang X, Li W, Li T-F, Li D-F. Aging, cell senescence, the pathogenesis and targeted therapies of osteoarthritis. Front Pharmacol 2021; 12: 728100.
5. Morrenti V, Benedetti F, Buriani A, Fortinguerra S, Caudullo G, Davinelli S, *et al.* Immunomodulatory and antiaging mechanisms of resveratrol, rapamycin, and metformin: Focus on mTOR and AMPK signaling networks. Pharmaceuticals 2022; 15: 912.
6. Glossmann HH, Lutz O. Metformin and aging: A review. Gerontology 2019; 65: 581-590.
7. Mohammed I, Hollenberg MD, Ding H, Triggle CR. A critical review of the evidence that metformin is a putative anti-aging drug that enhances healthspan and extends lifespan. Front Endocrinol 2021; 12: 718942.
8. Larsen MT, Kuhlmann M, Hvam ML, Howard KA. Albumin-based drug delivery: Harnessing nature to cure disease. Mol Cell Ther 2016; 4: 1-12.
9. Idrees H, Zaidi SZJ, Sabir A, Khan RU, Zhang X, Hassan S-u. A review of biodegradable natural polymer-based nanoparticles for drug delivery applications. Nanomaterials 2020; 10: 1970.
10. Tran X, Mulac D, Langer K. How to deliver an unselective drug selectively: Novel puromycin-loaded albumin nanoparticles for active targeting and their controllable effectiveness. J Drug Deliv Sci Technol 2025; 106: 106701.
11. Mishra D, Hubenak JR, Mathur AB. Nanoparticle systems as tools to improve drug delivery and therapeutic efficacy. J Biomed Mater Res A 2013; 101: 3646-3660.
12. Hong S, Choi DW, Kim HN, Park CG, Lee W, Park HH. Protein-based nanoparticles as drug delivery systems. Pharmaceutics 2020; 12: 604.
13. Wilson B, Paladugu L, Priyadarshini SB, Jenita JJL. Development of albumin-based nanoparticles for the delivery of abacavir. Int J Biol Macromol 2015; 81: 763-767.
14. Carvalho JR, Machado MV. New insights about albumin and liver disease. Ann Hepatol 2018; 17: 547-560.
15. Karimi M, Avci P, Mobasseri R, Hamblin MR, Naderi-Manesh H. The novel albumin–chitosan core–shell nanoparticles for gene delivery: Preparation, optimization and cell uptake investigation. J Nanopart Res 2013; 15: 1-14.
16. Frank LA, Onzi GR, Morawski AS, Pohlmann AR, Guterres SS, Contri RV. Chitosan as a coating material for nanoparticles

Corrected Proof

intended for biomedical applications. React Funct Polym 2020; 147: 104459.
17. Caprifico AE, Foot PJS, Polycarpou E, Calabrese G. Overcoming the protein corona in chitosan-based nanoparticles. Drug Discov Today 2021; 26: 1825-1840.
18. Lee C, Choi JS, Kim I, Oh KT, Lee ES, Park ES, *et al.* Long-acting inhalable chitosan-coated poly(lactic-co-glycolic acid) nanoparticles containing hydrophobically modified exendin-4 for treating type 2 diabetes. Int J Nanomedicine 2013; 8: 2975-2983.
19. Li J-m, Chen W, Wang H, Jin C, Yu X-j, Lu W-y, *et al.* Preparation of albumin nanospheres loaded with gemcitabine and their cytotoxicity against BXPC-3 cells *in vitro*. Acta Pharmacol Sin 2009; 30: 1337-1343.
20. Piazzini V, Landucci E, D'Ambrosio M, Fasiolo LT, Cinci L, Colombo G, *et al.* Chitosan coated human serum albumin nanoparticles: A promising strategy for nose-to-brain drug delivery. Int J Biol Macromol 2019; 129: 267-280.
21. Debacq-Chainiaux F, Erusalimsky JD, Campisi J, Toussaint O. Protocols to detect senescence-associated beta-galactosidase (SA-βgal) activity, a biomarker of senescent cells in culture and *in vivo*. Nat Protoc 2009; 4: 1798-1806.
22. Janero DR. Malondialdehyde and thiobarbituric acid-reactivity as diagnostic indices of lipid peroxidation and peroxidative tissue injury. Free Radic Biol Med 1990; 9: 515-540.
23.Senthilkumar M, Amaresan N, Sankaranarayanan A. Estimation of malondialdehyde (MDA) by Thiobarbituric Acid (TBA) Assay. In: Senthilkumar M, Amaresan N, Sankaranarayanan A, editors. Plant-Microbe Interactions: Laboratory Techniques. New York, NY: Springer US; 2021. p. 103-105.
24. Rahman I, Kode A, Biswas SK. Assay for quantitative determination of glutathione and glutathione disulfide levels using enzymatic recycling method. Nat Protoc 2006; 1: 3159-3165.
25. Guo J, Huang X, Dou L, Yan M, Shen T, Tang W, *et al.* Aging and aging-related diseases: From molecular mechanisms to interventions and treatments. Signal Transduct Target Ther 2022; 7: 391.
26. Cai Y, Song W, Li J, Jing Y, Liang C, Zhang L, *et al.* The landscape of aging. Sci China Life Sci 2022; 65: 2354-2454.
27. Balthasar S, Michaelis K, Dinauer N, von Briesen H, Kreuter J, Langer K. Preparation and characterisation of antibody modified gelatin nanoparticles as drug carrier system for uptake in lymphocytes. Biomaterials 2005; 26: 2723-2732.
28. Larsen MT, Kuhlmann M, Hvam ML, Howard KA. Albumin-based drug delivery: Harnessing nature to cure disease. Mol Cell Ther 2016; 4: 3.
29. Idrees H, Zaidi SZJ, Sabir A, Khan RU, Zhang X, Hassan SU. A review of biodegradable natural polymer-based nanoparticles for drug delivery applications. Nanomaterials (Basel) 2020; 10: 1970.
30. Hong S, Choi DW, Kim HN, Park CG, Lee W, Park HH. Protein-based nanoparticles as drug delivery systems. Pharmaceutics 2020; 12: 604.
31. He M, Fang M, Fan L, Maimaitijiang A. Preparation and characterization of BSA-loaded liraglutide and platelet fragment nanoparticle delivery system for the treatment of diabetic atherosclerosis. J Nanobiotechnology 2024; 22: 506.
32. Kong SZ, Li JC, Li SD, Liao MN, Li CP, Zheng PJ, *et al.* Anti-aging effect of chitosan oligosaccharide on d-galactose-induced subacute aging in mice. Mar Drugs 2018; 16: 181.
33. Salim EI, Abd El Khalik EAM, Shalaby TI, Ali EMM. Synthesis, characterisation and enhanced apoptotic effect of gemcitabine-loaded albumin nanoparticles coating with chitosan. Arch Physiol Biochem 2022; 128: 970-978.
34. Kong SZ, Li DD, Luo H, Li WJ, Huang YM, Li JC, *et al.* Anti-photoaging effects of chitosan oligosaccharide in ultraviolet-irradiated hairless mouse skin. Exp Gerontol 2018; 103: 27-34.
35. Malaiya A, Kenwat R, Mamgain A, Nayak P, Parker A, Paliwal SR, *et al.* Intranasal resveratrol delivery to the brain with chitosan-decorated bovine serum albumin nanoparticles: Advancing Alzheimer's management in old female rats through QbD-based optimization, *in vitro* evaluation, and *in vivo* exploration. Int J Biol Macromol 2025; 311: 143300.
36. Taherian A, Esfandiari N, Rouhani S. Breast cancer drug delivery by novel drug-loaded chitosan-coated magnetic nanoparticles. Cancer Nanotechnology 2021; 12: 15.
37. Esim O, Oztuna A, Sarper M, Hascicek C. Chitosan-coated bovine serum albumin nanocarriers mediate efficient delivery of methotrexate in breast cancer therapeutics. J Drug Deliv Sci Technol 2022; 77: 103906
38. Piazzini V, Landucci E, D'Ambrosio M, Tiozzo Fasiolo L, Cinci L, Colombo G, *et al.* Chitosan coated human serum albumin nanoparticles: A promising strategy for nose-to-brain drug delivery. Int J Biol Macromol 2019; 129: 267-280.
39. Karimi M, Avci P, Mobasseri R, Hamblin MR, Naderi-Manesh H. The novel albumin–chitosan core–shell nanoparticles for gene delivery: Preparation, optimization and cell uptake investigation. J Nanopart Res 2013; 15: 1651.
40. Radwan SE-S, El-Moslemany RM, Mehanna RA, Thabet EH, Abdelfattah E-ZA, El-Kamel A. Chitosan-coated bovine serum albumin nanoparticles for topical tetrandrine delivery in glaucoma: *In vitro* and *in vivo* assessment. Drug Deliv 2022; 29: 1150-1163.
41. Bessone F, Dianzani C, Argenziano M, Cangemi L, Spagnolo R, Maione F, *et al.* Albumin nanoformulations as an innovative solution to overcome doxorubicin chemoresistance. Cancer Drug Resistance 2021; 4: 192.
42. Li Y, Song H, Xiong S, Tian T, Liu T, Sun Y. Chitosan-stablized bovine serum albumin nanoparticles having ability to control the release of NLS protein. Int J Biol Macromol 2018; 109: 672-680.
43. Jose J, Sundar K, Anjali C, Ravindran A. Metformin-loaded BSA nanoparticles in cancer therapy: A new perspective for an old antidiabetic drug. Cell Biochem biophys 2015; 71:627-636.
44. Hasan M, Belhaj N, Benachour H, Barberi-Heyob M, Kahn CJ, Jabbari E, *et al.* Liposome encapsulation of curcumin: Physico-chemical characterizations and effects on MCF7 cancer cell proliferation. Int J Pharm 2014; 461: 519-528.
45. Shin GH, Chung SK, Kim JT, Joung HJ, Park HJ. Preparation of chitosan-coated nanoliposomes for improving the mucoadhesive property of curcumin using the ethanol injection method. J Agric Food Chem 2013; 61: 11119-11126.
46. Kumari A, Yadav SK, Yadav SC. Biodegradable polymeric nanoparticles based drug delivery systems. Colloids Surf B Biointerfaces 2010; 75: 1-18.
47. Agnihotri SA, Mallikarjuna NN, Aminabhavi TM. Recent advances on chitosan-based micro- and nanoparticles in drug delivery. J Control Release 2004; 100: 5-28.
48. Lertsutthiwong P, Noomun K, Khunthon S, Limpanart S. Influence of chitosan characteristics on the properties of biopolymeric chitosan–montmorillonite. Progress Nat Sci Mater Int 2012; 22: 502-508.
49. Prego C, García M, Torres D, Alonso MJ. Transmucosal macromolecular drug delivery. J Control Release 2005; 101: 151-162.
50. Dimri GP, Lee X, Basile G, Acosta M, Scott G, Roskelley C, *et al.* A biomarker that identifies senescent human cells in culture and in aging skin in vivo. Proc Natl Acad Sci U S A 1995; 92: 9363-9367.
51. Aibani N, Rai R, Patel P, Cuddihy G, Wasan EK. Chitosan nanoparticles at the biological interface: Implications for drug delivery. Pharmaceutics 2021; 13: 1686.
52. Fukuzawa K, Saitoh Y, Akai K, Kogure K, Ueno S, Tokumura A, *et al.* Antioxidant effect of bovine serum albumin on membrane lipid peroxidation induced by iron chelate and superoxide. Biochim Biophys Acta 2005; 1668: 145-155.
53. Chang HT, Cheng H, Han RM, Zhang JP, Skibsted LH. Binding to bovine serum albumin protects β-carotene against oxidative degradation. J Agric Food Chem 2016; 64: 5951-5957.
54. Ye J, Bounds A, Crumpton M, Long M, McDonough H, Srikhirisawan I, *et al.* Potential mechanisms of lactate dehydrogenase and bovine serum albumin proteins as antioxidants: A mixed experimental-computational study. Biochem Res Int 2025; 2025: 9638644.
55. Ngo DH, Kim SK. Antioxidant effects of chitin, chitosan, and

Corrected Proof

their derivatives. Adv Food Nutr Res 2014; 73: 15-31.
56. Shang S, Li X, Wang H, Zhou Y, Pang K, Li P, *et al.* Targeted therapy of kidney disease with nanoparticle drug delivery materials. Bioact Mater 2024; 37: 206-221.
57. Chen S, Gan D, Lin S, Zhong Y, Chen M, Zou X, *et al.* Metformin in aging and aging-related diseases: Clinical applications and relevant mechanisms. Theranostics 2022; 12: 2722-2740.

Corrected Proof